DIRECT NUMERICAL SIMULATIONS OF TURBULENT BOUNDARY LAYERS OVER SQUARE-EDGED 2-D AND 3-D ROUGH WALLS

Jae Hwa Lee and Hyung Jin Sung*
Department of Mechanical Engineering,
KAIST
373-1 Guseong-dong, Yuseong-gu, Daejeon, 305-701, Korea
jhlee06@kaist.ac.kr, leehuiso@kaist.ac.kr, hjsung@kaist.ac.kr*

ABSTRACT

Direct numerical simulations (DNSs) of spatially developing turbulent boundary layers (TBLs) over two-dimensional (2-D) rod- and three-dimensional (3-D) cube-roughened walls were performed to see the roughness effects on the properties of TBL. The 2-D and 3-D roughness were periodically arranged in the downstream direction with pitches of p_x/k=2, 3, 4, 6, 8 and 10 and, for the cube the spanwise spacing is fixed at p_z/k=2 with staggered array, where p_x and p_z are the streamwise and spanwise spacings of the roughness and k is the roughness height. Inspection of the Reynolds stresses showed that except for p_x/k=2 and 3 over the 2-D rough walls, the effects of the surface roughness extend to the outer layer over the 2-D and 3-D rough walls and the magnitude of the Reynolds stresses in the outer layer is increased in proportion to p_x/k. The consistent results were observed in the behavior of wall-normal fluctuations (v_w^+) on the crest of the roughness suggested by Orlandi & Leonardi (2008), indicating that v_w^+ might be a suitable parameter to predict the influence of the surface roughness in the outer layer over the square-edged rough walls. However, such results are contrary to the trends of the form drag, roughness function and roughness length against p_x/k, which showed the maximum values at p_x/k=8 and 4 over the 2-D and 3-D rough walls respectively.

INTRODUCTION

Townsend's wall-similarity hypothesis (1976) states that outside the roughness sublayer turbulent motions are independent of the surface roughness, and that the interaction between the inner and outer layers is very weak at a sufficiently large Reynolds number. In an effort to support this hypothesis, a number of studies with rough walls have been performed until now. Schultz & Flack (2005) and their subsequent papers in rough-wall turbulent boundary layers showed the satisfaction of the outer layer-similarity and especially, their recent experiment study of Flack *et al.* (2007) using 3-D mesh and sandpaper with a large range of roughness heights revealed that there is no critical roughness height and that the effects of roughness are confined to a roughness sublayer of $5k$ or $3k_s$, where k_s is the equivalent sand-grain height, even when larger roughness are used. These results indicate that in the TBLs with irregular shapes of 3-D roughness having sufficient small and large sizes, the outer-layer similarity is established in the regions of $y>5k$ or $y>3k_s$ at high Reynolds numbers.

However, the results from several experimental and numerical studies of TBLs over surfaces with restricted 2-D rod roughness showed that the effects of the roughness extend to the outer layer at both low and high Reynolds numbers regardless of the roughness height (Krogstad & Antonia 1999; Lee & Sung 2007; Volino *et al.* 2009; Volino *et al.* 2011). These previous results suggest that the 2-D roughness affects the boundary layer differently from the 3-D roughness and the wall-similarity and its necessary conditions may not be universal for the given flow types (Snyder & Castro 2002) and additionally, it plausibly seems to be related to other factors, e.g. dimensions of roughness and geometric shapes, etc.

Recently, Lee *et al.* (2011) carried out the DNS of a spatially developing TBL over a wall roughened with regularly arrayed cubes to examine the influences of the dimensional variations. They changed the geometric shape from the transverse 2-D bar of Lee & Sung (2007) to the 3-D cubes by chopping the rod in the spanwise direction (p_z/k=2). The cubes were periodically staggered in the downstream, while maintaining the streamwise spacing of p_x/k =8. They found that the cube roughness also affects the turbulent Reynolds stresses not only in the roughness sublayer but also in the outer layer, though the strength is weaker than the 2-D rod roughness. Lee *et al.* (2011) concluded that the failure of the wall-similarity in the outer layer might be induced by the long streamwise extent of the arranged 2-D and 3-D roughness elements and the square planes of roughness or either of the two, which results in strong blockage effects that create active upward motions.

For the turbulent channel flow with transverse square bars on one wall, the effects of the streamwise extent of the 2-D bar roughness have been examined by Leonardi *et al.* (2003). They showed that the minimum skin-friction drag and the maximum form drag occur at p_x/k=8. However, there is obvious difference between channel flows and boundary layers, at least in the outer region (Krogstad *et al.* 2005; Volino *et al.* 2009; Lee *et al.* 2011).

The aim of the present paper is to investigate the effects of the streamwise spacing on the interaction between inner and outer layers in the TBLs and the limited distance to expect the wall-similarity in the outer layer. In addition, if possible, we wish to find suitable parameter to predict the establishment of the wall-similarity in the outer layer over the square-edged rough walls. Large amounts of DNSs of the TBLs over walls roughened with regularly arrayed 2-D rods and 3-D cubes were carried out with p_x/k=2, 3, 4, 6, 8 and 10. For the cube roughness, the spanwise extent between the cubes was fixed at p_z/k=2 in the present study.

We first examined how the flow parameters vary at the similar Reynolds number against p_x/k over the 2-D and 3-D rough walls. The profiles of the mean and Reynolds stresses were compared and various parameters were extracted to quantify the effects of turbulent rough flows, such as the roughness function (ΔU^+) and root mean square of the normal velocity fluctuations at the plane of the crests (v_w^+) suggested by Orlandi & Leonardi (2008) in the turbulent channel flow.

NUMERICAL METHOD

For an incompressible flow, the nondimensional governing equations are

$$\frac{\partial u_i}{dt} + \frac{\partial u_i u_j}{\partial x_j} = -\frac{\partial p}{\partial x_i} + \frac{1}{\mathrm{Re}}\frac{\partial^2 u_i}{\partial x_j \partial x_j} + f_i \quad (1)$$

$$\frac{\partial u_i}{\partial x_i} = 0 \quad (2)$$

where x_i are the Cartesian coordinates and u_i are the corresponding velocity components. The governing equations are integrated in time by using the fractional step method with the implicit velocity decoupling procedure proposed by Kim *et al.* (2002). Based on a block LU decomposition, both the velocity-pressure decoupling and the additional decoupling of intermediate velocity components are achieved through approximate factorization. The immersed boundary method was used to describe the roughness elements with Cartesian coordinates and a rectangular domain (Kim *et al.* 2001). The discrete-time momentum forcing f_i was calculated explicitly in time to satisfy the no-slip condition at the immersed boundary by using the previous velocity field near the forcing point.

The notational convention adopted is that x, y, and z denote the streamwise, vertical, and spanwise coordinates, respectively, and that u, v, and w denote the streamwise, wall-normal, and spanwise components of the velocity fluctuations, respectively. Since the boundary layer is developing spatially in the downstream direction, it is necessary to use non-periodic boundary conditions in the streamwise direction. To avoid generating a rough-wall inflow, which is prohibitively difficult, the first element was placed $80\theta_{in}$ downstream from the inlet; the surface condition changes abruptly from smooth to rough at this location, which was defined as x=0. Therefore, the domain size should be sufficiently long for the flow to reach a new equilibrium state, which results in self-preservation in the computational domain. The inflow data obtained from the auxiliary simulations based on the method of Lund *et al.* (1998) was employed in the present study. Lee & Sung (2007) and Lee *et al.* (2011) showed that the resulting turbulence statistics of the mean velocity and Reynolds stresses at Re_θ=300 are in good agreement with those of Spalart (1988) over the 2-D rod- and 3-D cube-roughened walls. At the exit, the convective boundary condition was specified as $(\partial u/\partial t)+c(\partial u/\partial x)$ =0, where c is the local bulk velocity. The no-slip boundary condition was imposed at the solid wall, and the boundary layer conditions on the top surface of the computational domain were $u=U_\infty$ and $\partial v/\partial y=\partial w/\partial y$=0. Periodic boundary conditions were applied in the spanwise direction.

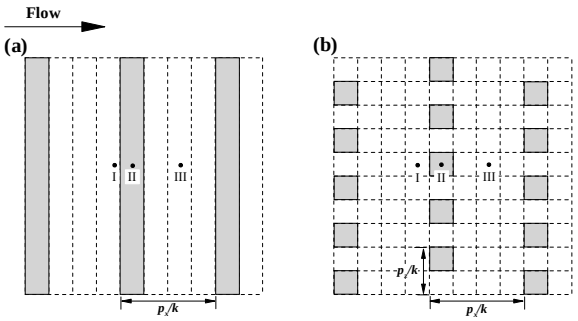

Figure 1: Schematic top views of the small parts of the whole computational domains. (a) 2-D and (b) 3-D rough walls with the streamwise spacing p_x/k=4. These parts are repeated in the horizontal direction and the flow direction is from left to right.

Figure 1 shows schematic views of the small parts of the computational domains over the 2-D and 3-D rough walls. The streamwise spacing is p_x/k=4 for both cases and these patterns are repeated in the streamwise and spanwise directions respectively. In the present work, total of thirteen simulations including six 2-D rod cases, six 3-D cube cases and the smooth wall case were compared with the variation of the streamwise spacing p_x/k. For the 3-D cube roughness, the arrays are staggered in the streamwise direction and the pitch of the spanwise distance is fixed at p_z/k=2. All roughness heights (k) are the same as $k=1.5\theta_{in}$, when normalized by the inlet momentum thickness (θ_{in}). In the present study, since the profiles of all the flow statistics are collapsed above the roughness sublayer $y=5k$ and especial attention is paid to the outer region, we presented the results at the representative location III, as shown in figure 1.

Results and discussion

Figure 2 exhibits the spatial averaged skin-friction (C_f) and form drags (C_p) against p_x/k over the 2-D and 3-D rough walls at the similar Reynolds number $Re_\theta \simeq 1100$. As can be seen, in the TBLs over 2-D rod-roughened walls, the skin-friction drag is significantly affected by p_x/k. The maximum value is observed at p_x/k=2 and as p_x/k increases, the values of the skin-friction drag are decreased, because the strength of the recirculation becomes stronger. In the region at p_x/k=2, the frictional contributions to the total drag are not negligible, and thus all the drag arises from both frictional and pressure drags acting on the roughness elements, implying the transitional rough at which viscous effects are not negligible. Therefore, the 2-D rough wall flow with p_x/k=2 is in transitional regime. This result is consistent with that of Ligrani & Moffat (1986). For the range $p_x/k \geq 5$, the skin-friction drag has a negative value due to the induction of the large recirculation region between the transverse rods and the minimum occurs at p_x/k=8. For the 3-D cube-roughened walls, however, the skin-friction drag is always positive due to that the backflow regions which contributes to create the negative skin-friction drag are confined to a narrow region near the cubes and the minimum occurs at p_x/k=4.

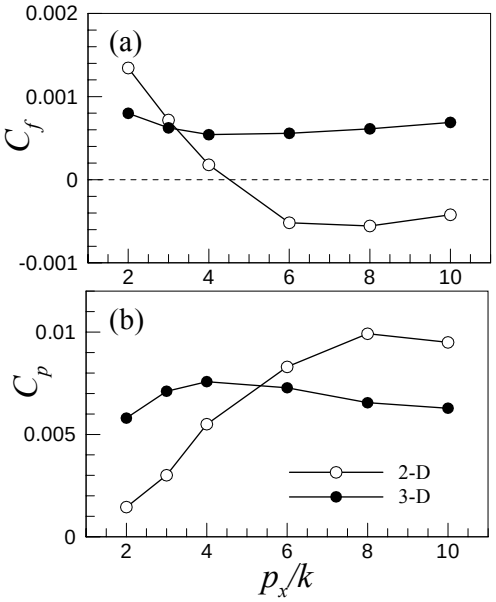

Figure 2: Variations of skin-friction (C_f) and form drag (C_p) with respect to p_x/k over the 2-D and 3-D rough walls.

In addition, it is clearly shown that over the square-edged rough walls with various p_x/k, the form drag is much larger than the skin-friction drag, except for the 2-D rough wall at p_x/k=2, implying the fully rough regime at which the form drag is a dominant contributor to total drag. Consistent with those of the skin-friction drag, the form drag over the 3-D rough walls has a weak dependence on p_x/k and there is approximately 30% difference between the maximum (at p_x/k=4) and minimum (at p_x/k=2) values. For the 2-D rough walls, however, the maximum value at p_x/k=8 is more than six times larger than the minimum value at p_x/k=2, showing the strong dependency on p_x/k. The form drag increases rapidly over the range $2<p_x/k<4$ and it becomes moderate for $6<p_x/k<10$, with a weak maximum at p_x/k=8. This trend is similar to the previous experimental and numerical studies over the 2-D rough wall cases by Furuya *et al.* (1976) and Leonardi *et al*. (2003). In addition, it is worth mentioning that the effects of the 2-D rough walls are not always stronger than those of the 3-D rough walls. For $p_x/k<6$, the form drag is larger over the 3-D rough walls, because the flow diverted laterally between roughness speeds up in the gap and creates to greater pressure on the front of the cubes. Over the 2-D rough walls at small p_x/k, however, the flow slowly recirculates and the reattachment takes place on the next roughness, leading to weak form drag at the leading edge of the roughness. The reverse is true for $p_x/k\geq6$. The flow over the 2-D rough walls is separated at the leading edge of the roughness and reattached to the bottom wall. This flow impinges to the next roughness and forms the much stronger pressure than the 3-D rough walls.

Figure 3 shows the variations of the friction velocity (u_τ/U_∞) with respect to p_x/k over the 2-D and 3-D rough walls. The friction velocity can be directly estimated from the total drag, which is sum of the skin-friction and form drags. This represents a strong advantage of DNS over experiment, since there is no ambiguity, regarding the

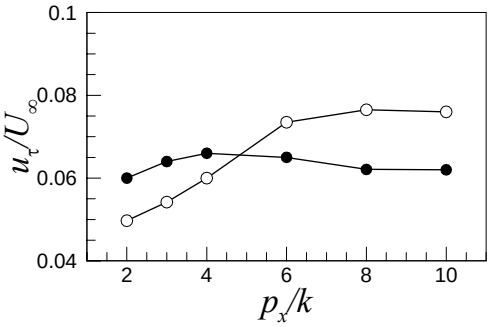

Figure 3: Variations of the friction velocity (u_τ/U_∞) with respect to p_x/k over the 2-D and 3-D rough walls.

various parameters to fit. Because the magnitudes of the form drag are much larger than the skin-friction drag over the 2-D and 3-D rough walls, the overall shapes of the curves are similar to those of the form drag. However, the gap of the form drags between the 2-D and 3-D rough walls p_x/k=2 is apparently reduced owing to the contribution of maximum skin-friction drag positively to the friction velocity. Compared to the smooth wall, the friction velocity is increased up to 6~65% and 28~41% over the 2-D and 3-D rough walls with varying p_x/k respectively, indicating that the nature for different behavior between smooth and rough flows relies on the friction on the surface; only viscous drag is present for the smooth wall, whereas the form drag prevails over the viscous drag for the rough walls.

It is interesting that the streamwise pitch at which the maximum of the form drag and friction velocity over the 3-D rough walls occurs is actually the same as the 2-D rough wall at p_x/k=8, because of the staggered array of the cubes, as shown in figure 1, implying the possibility that the streamwise spacing between the roughness aligned in the straight manner is an important parameter to affect the friction, although there are staggered arrays of the cubes in the spanwise direction. However, the reason why the maximum occurs at p_x/k=4 over the 3-D rough wall which has the density of 12.5% might be explained by the density of the roughness, studied by Leonardi & Castro (2010). They examined the channel flow with rough walls comprising staggered arrays of cubes having various plan area densities and found that the surface drag is predominantly a form drag and the maximum contribution occurs at an area coverage around 15% (at approximately p_x/k=2.75). Note that their roughness configuration is slightly different from the present study. In their study, the cubes were lined up in the spanwise direction, but staggered in the streamwise direction and with each cube positioned centrally between the two nearest upstream cubes (see figure 1 in their paper). These results indicate that for the staggered arrays of the cubes, the friction is significantly affected by the densities rather than the arrays (p_x/k) of the roughness and the streamwise spacing at p_x/k=4 over the 3-D rough wall is incidentally the same as that of the 2-D rough wall at p_x/k=8 in the straight manner.

The effect of surface roughness on the velocity distribution of the TBL can be expressed in the following form with inclusion of the virtual origin:

$$U^+ \equiv \frac{U}{u_\tau} = \frac{1}{\kappa}\ln\left(\frac{y'u_\tau}{\nu}\right) + B - \Delta U^+ \qquad (3)$$

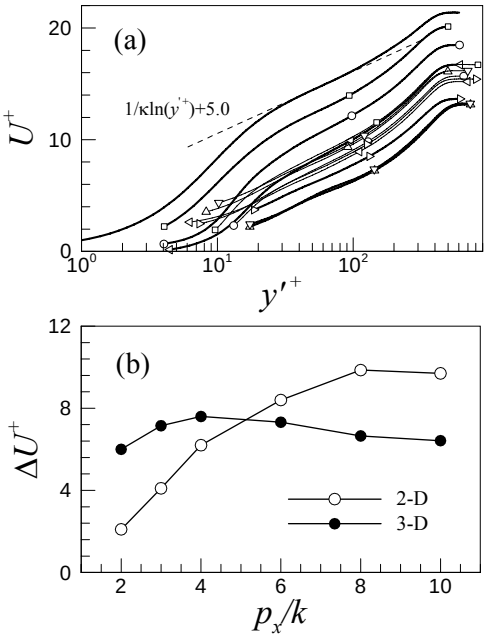

Figure 4: (a) Mean streamwise velocity profiles and (b) variation of the roughness function (ΔU^+). Each case is distinguished using a single symbol with different line thickness.

where the capital U denotes the time-averaged quantity, y' is y-ε, κ is the Kármán constant, B is a smooth wall additive constant, ε is the virtual origin and ΔU^+ is the roughness function. Variables with a + superscript are expressed in wall units, using the friction velocity, u_τ and viscous length ν/u_τ. The mean velocity profiles at location III over the 2-D and 3-D rough walls are shown in figure 4(a). The bold solid lines with the symbols represent the results from the 2-D rough walls and the thin solid lines are visible for the 3-D rough walls. With the usual inner scaling, all the profiles are shifted below the standard log-law line, as expected.

The variation of the roughness function (ΔU^+) with respect to p_x/k is summarized in figure 4 (b) over the 2-D and 3-D rough walls. The maximum shifts occur at p_x/k=8 and 4 over the 2-D and 3-D rough walls, i.e. the geometries yielded the maximum values of the form drag. This distribution is very similar to that of the form drag rather than the friction velocity. The implication is that the pressure difference around the roughness element influences ΔU^+ directly and the skin-friction drag has a weak effect on ΔU^+. The consistent results are reported in the previous experimental and numerical studies of Furuya *et al.* (1976) and Leonardi *et al.* (2003) over the 2-D rough walls. However, large differences between the present values of ΔU^+ and those of the previous results are found. These discrepancies might be attributed to that the geometry of Furuya *et al.* (1976) and the size of the roughness of Leonardi *et al.* (2003) differ from the present work and possibly, there might be a difference between internal and external flows.

Reynolds stresses in the outer coordinates normalized by the friction velocity are shown for the 2-D and 3-D rough walls in figures 5 and 6 along with the smooth wall. Over the 2-D rough walls, the streamwise normal stresses u_{rms}^{+2} in the roughness sublayer have the maximum around y'+=15 at small p_x/k, which would be expected in boundary

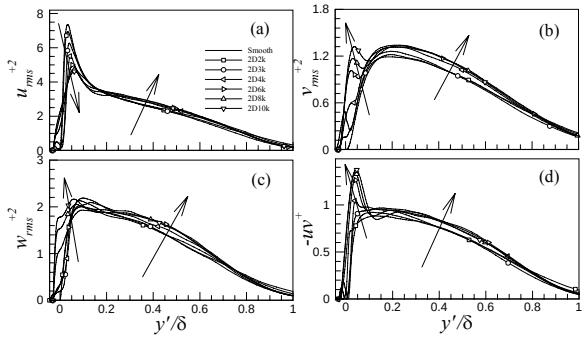

Figure 5: Reynolds stresses over the 2-D rough walls in the outer coordinates.

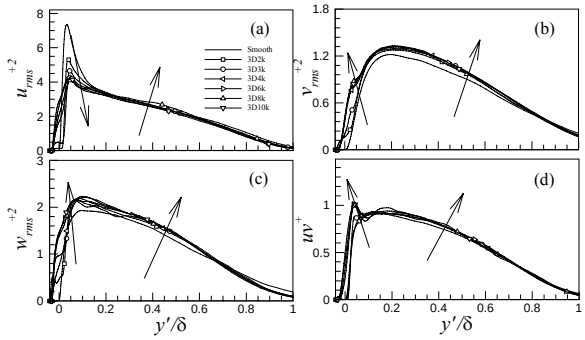

Figure 6: Reynolds stresses over the 3-D rough walls in the outer coordinates.

layers developing over a smooth wall. As p_x/k increases, the peak values are decreased and especially it is more obvious in variation at small p_x/k. Note that the peak value is the lowest at p_x/k=10. For the 3-D rough walls, however, the variation of the near-wall peaks is not significant against p_x/k and the minimum value occurs at p_x/k=10. In the near-wall plots of the wall-normal v_{rms}^{+2}, spanwise w_{rms}^{+2} and Reynolds shear stress uv^+ components, the reverse behaviors are shown to those of streamwise component that the peaks in the near-wall region are increased with increasing p_x/k over the 2-D and 3-D rough walls. The turbulent energy is transferred from the streamwise direction to wall-normal and spanwise directions. This distribution of turbulent kinetic energy is very similar to that of DNS for rough-wall channel flow by Ashrafian & Andersson (2006).

In the outer layer (y>5k), the profiles of the Reynolds stresses over the 2-D rough walls with p_x/k=2 and 3show an excellent agreement with the smooth wall, implying very weak interaction between inner and outer layers. However, other cases over the 2-D and 3-D rough walls show that the outer layer is significantly affected by the surface roughness, regardless of p_x/k. In addition, careful inspection of the outer region (at y'/δ=0.4) reveals that the magnitude of the outer peak for the Reynolds stresses, in particular the wall-normal and spanwise components, is increased with increasing p_x/k. These behaviors are contrary to the previous flow statistics which showed that the maximum values occur at p_x/k=8 and 4 over the 2-D and 3-D rough walls. The implication of the present results is that the Reynolds stresses in the outer layer is not perfectly correlated to the flow statistics, such as the form drag, roughness function and so on, and these are closely associated with the streamwise spacing over the square-edged rough walls. Comparison of the maximum values between the rough and

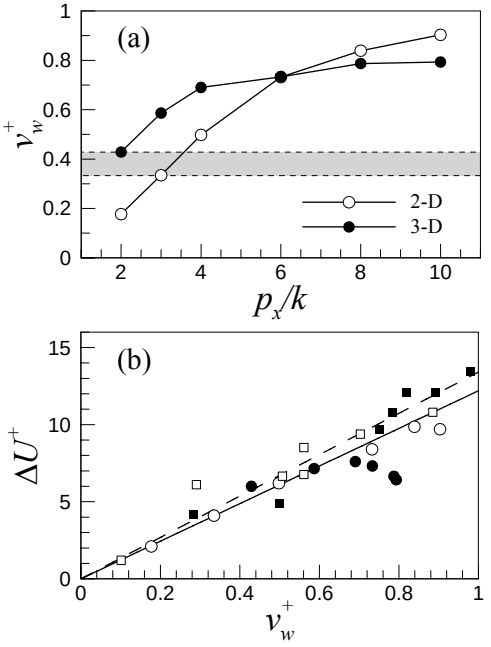

Figure 7: Variations of (a) wall-normal fluctuations (v_w^+) at the plane of the roughness crests versus the streamwise spacing and (b) roughness functions (ΔU^+) versus v_w^+. ○, 2-D; ●, 3-D; □, Orlandi & Leonardi (2006); ■, Orlandi & Leonardi (2008); solid line, $\Delta U^+ = B/\kappa v_w^+$ $(B = 5.0)$; dashed line, $\Delta U^+ = B/\kappa v_w^+$ $(B = 5.5)$.

smooth walls shows more increased values over the 2-D rough wall and these increases are estimated to be higher approximately 7% for the 3-D rough walls and 13% for the 2-D rough walls than over the smooth wall. In sum, we can conclude that the streamwise spacing which yields the maximum outer peak is p_x/k =10 over the 2-D and 3-D rough walls respectively, and this is not consistent with those of the previous flow statistics. In the turbulent channel flow with square-edged rough wall, however, the profiles of the Reynolds stresses collapse well with that of the smooth wall in the outer layer, in conformity with Townsend's hypothesis that the only effect of roughness is to change the near-wall surface stress (Krogstad *et al.* 2005; Leonardi & Castro 2010).

Finally, it is worth seeking for a parameter to investigate the possibility for determining the wall-similarity in the outer layer. The previous results showed that although the maximum contribution to the form drag, roughness function and roughness length occur at 2D8k and 3D4k, the streamwise spacing at which maximum contribution to the Reynolds stresses occurs in the outer layer is p_x/k=10 over the 2-D and 3-D rough walls. Therefore, it is not appropriate to parameterize the form drag and roughness function, etc for estimation of the outer-layer similarity in TBL and at this point, it is necessary to employ a new parameter for prediction of the outer-layer effects. Orlandi & Leonardi (2008) tried to find a new parameterization for turbulent rough flows and showed that large variations of drag and turbulence production are linked to the wall-normal fluctuations (v_w^+) on the crest of the roughness.

Figure 7(a) shows the variations of v_w^+ with respect to p_x/k over the 2-D and 3-D rough walls. The results show monotonous increase with increasing p_x/k and especially at large p_x/k over the 3-D rough walls, the trend is obviously different from those of the form drag and roughness function. These results are entirely consistent with that of the Reynolds stresses in the outer layer and show that the wall-normal fluctuations on the crest of the roughness are proportional to p_x/k over the square-edged 2-D and 3-D rough walls. In addition, it is shown that beyond the certain limit of v_w^+ depicted by grey band, the effects of the surface roughness are observed to extend to the outer layer and in the range of less than approximately 0.4, a weak interaction between inner and outer layers is expected. In our opinion, therefore, there is strong correlation between wall-normal fluctuations and Reynolds stresses in the outer layer and the parameter v_w^+ might be a suitable candidate to estimate the inner and outer layers interaction and their strength over the square-edged rough wall TBLs.

Figure 7(b) shows the variation of ΔU^+ with respect to v_w^+. Orlandi & Leonardi (2008) proposed a simple expression $\Delta U^+ = \frac{B}{\kappa} v_w^+$ between ΔU^+ and v_w^+. As similar to that of Orlandi & Leonardi (2008) in the turbulent channel flow, the results over the 2-D rough walls show a linear relation between them and collapse well with the correlation of B=5.0, even at large v_w^+. However, the data over the 3-D rough walls show a slight discrepancy through the entire range, in particular, at large v_w^+. Leonardi & Castro (2010) reported the similar behavior to the present study. They found that for 3-D roughness arrays the normal stress falls monotonically with increasing the area density of roughness (with decreasing p_x/k), although the roughness function has a peak value at around 15% of the area density. These differences indicate that there is limitation to predict the roughness function over the 3-D rough walls using the normal Reynolds stress on the roughness crest, because v_w^+ is strongly proportional to p_x/k even over the 3-D rough walls, but ΔU^+ is associated with the density under the staggered arrays of the cubes.

CONCLUSIONS

The DNSs of the spatially developing TBLs over rod- and cube-roughened walls were performed to investigate the effects of the streamwise spacing on its turbulence statistics and coherent structures. Inspection of the flow statistics of the form drag, the friction velocity and the roughness function over the 2-D rough walls showed that these quantities are strongly dependent on p_x/k and the maximum and minimum values occur at p_x/k=8 and 2 respectively. However, the results from the 3-D rough walls showed the relatively weak dependency on p_x/k than those of the 2-D rough walls and the maximum contribution to the friction was observed at p_x/k=4. These results over the 3-D rough walls indicated that the effects of the surface roughness are significantly influenced by the densities than the arrays of the cubes under the staggered arrays of the cubes.

The profiles of the Reynolds stresses over the 2-D and 3-D rough walls showed that although there is little

interaction between inner and outer layers over the 2-D rough walls at p_x/k=2 and3, the effects of the surface roughness for other cases are observed in the outer layer. We found that the behavior over the 3-D rough walls is contrary to the previous observations over the irregular 3-D roughness including mesh, sandpaper and others, which showed the outer-layer similarity, while the values of k_s/k in the present study are similar to the previous ones. These differences are attributable to the effects of the geometric shape that the sparsely distributed cubes with square planes induce strong blockage effects that the consistent with those of the 2-D rod-roughened walls. In addition, the outer peak values in the Reynolds stresses are increased with increasing p_x/k and the streamwise spacing which yields the maximum outer peak is p_x/k=10 over the 2-D and 3-D rough walls. Such results are obviously distinguishable to the turbulent channel flow with square-edged rough walls which shows an excellent agreement with that of the smooth wall in the outer layer, in conformity with Townsend's hypothesis that the only effect of roughness is to change the near-wall surface stress.

Since the characteristic of the Reynolds stresses in the outer layer is different from those of the flow statistics related to the friction, it is worth seeking for a new parameter to estimate the interaction between inner and outer layers. In the present study, we found that the wall-normal fluctuations (v_w^+) on the crest of the roughness are closely associated to the behavior of the Reynolds stresses in the outer layer and it is proportional to p_x/k over the square-edged 2-D and 3-D rough walls. In addition, the results showed that there is a critical value of v_w^+ to expect the weak interaction between inner and outer layers, indicating that the parameter v_w^+ might be a suitable candidate to predict the outer-layer similarity and their possible strength over the square-edged rough wall TBLs.

ACKNOWLEDGEMENT

This work was supported by the Creative Research Initiatives (No. 2011-0000423) of the National Research Foundation of Korea.

REFERENCES

Ashrafian, A., & Andersson, H. I., 2006, "Roughness effects in turbulent channel flow," *Prog. Comput. Fluid Dyn*. 6, 1-20.

Flack, K. A., Schultz, M. P., & Connelly, J. S., 2007, "Examination of a critical roughness height for outer layer similarity," *Phys. Fluids* 19, 095104.

Furuya, Y., Miyata, M., Fujita, H., 1976, "Turbulent boundary layer and flow resistance on plates roughened by wires," *Trans. ASME: J. Fluids Engng* 98, 635-644.

Kim, J., Kim, D., & Choi, H., 2001, "An immersed boundary finite-volume method of simulations of flow in complex geometry," *J. Comput, Phys* 171, 132-150.

Kim, K., Baek, S. –J., and Sung, H. J., 2002, "An implicit velocity decoupling procedure for the incompressible Navier-Stokes equations," *Intl J Numer Meth Fluids* 38, 125-138.

Krogstad, P. -Å., Andersson, H. I., Bakken, O. M., & Ashrafian, A., 2005, "An experimental and numerical study of channel flow with rough walls," *J. Fluid Mech* 530, 327-352.

Krogstad, P. -Å., & Antonia, R. A., 1999, "Surface roughness effects in turbulent boundary layers," *Exp. Fluids* 27, 450-460.

Lee, J. H., Sung, H. J., & Krogstad, P. -Å., 2011, "Direct numerical simulation of the turbulent boundary layer over a cube-roughened wall," *J. Fluid Mech* 669,397-431.

Lee, S. –H., & Sung, H. J., 2007, "Direct numerical simulation of the turbulent boundary layer over a rod-roughened wall," *J. Fluid Mech* 584, 125-146.

Leonardi, S., & Castro, P., 2010, "Channel flow over large cube roughness: a direct numerical simulation study," *J. Fluid Mech* 651, 519-539.

Leonardi, S., Orlandi, P., Smalley, R. J., Djenidi, L., & Antonia, R. A., 2003, "Direct numerical simulations of turbulent channel flow with transverse square bars on one wall," *J. Fluid Mech* 491, 229-238.

Ligrani, P. M., & Moffat, R. J., 1986, "Structure of transitionally rough and fully rough turbulent boundary layers," *J. Fluid Mech* 162, 69-98.

Lund, T. S., Wu, X., & Squires, K. D., 1998, "Generation of turbulent inflow data for spatially-developing boundary layer simulation," *J. Comput, Phys* 140, 233-258.

Orlandi, P., & Leonardi, S., 2008, "Direct numerical simulation of three-dimensional turbulent rough channels: parameterization and flow physics," *J. Fluid Mech* 606, 399-415.

Schultz, M. P., & Flack, K. A., 2005, "Outer layer similarity in fully rough turbulent boundary layers," *Exp. Fluids* 38, 328-340.

Snyder, W. H., & Castro, I. P., 2002, "The critical Reynolds number for rough-wall boundary layers," J. *Wind Engng Indus. Aerodyn*. 90, 41-54.

Spalart, P. R., 1988, "Direct simulation of a turbulent boundary layer up to Re_θ=1410," *J. Fluid Mech*. 187, 61-98.

Volino, R. J., Schultz, M. P., & Flack, K. A., 2009, "Turbulent structure in a boundary layer with two-dimensional roughness," *J. Fluid Mech* 625, 75-101.

Volino, R. J., Schultz, M. P., & Flack, K. A., 2011, "Turbulent structure in boundary layers over periodic two- and three-dimensional roughness," *J. Fluid Mech* (to appear).

Townsend, A. A., 1976, "The structure of turbulent shear flow," p. 429. Cambridge University Press.